Influence of β-$FeSi_2$ particle size and Si growth rate on 1.5 μm photoluminescence from Si/β-$FeSi_2$-particles/Si structures grown by molecular-beam epitaxy

Y. Ozawa and T. Ohtsuka
Institute of Applied Physics, University of Tsukuba, Tsukuba, Ibaraki 305-8573, Japan

Cheng Li, T. Suemasu, and F. Hasegawa
Institute of Applied Physics and Center for Tsukuba Advanced Research Alliance, University of Tsukuba, Tsukuba, Ibaraki 305-8573, Japan

(Received 24 November 2003; accepted 24 February 2004)

Si/β-$FeSi_2$-particles/Si structures have been fabricated by reactive deposition epitaxy for β-$FeSi_2$ and molecular-beam epitaxy (MBE) for Si, and the influence of the size of the β-$FeSi_2$ particle and the MBE-Si growth rate for embedding the β-$FeSi_2$ in Si on 1.5-μm photoluminescence (PL) intensity of β-$FeSi_2$ was investigated. The 1.5-μm PL intensity was observed to increase with the size of the β-$FeSi_2$ particle, but the broad background luminescence, ranging from 1.2 to 1.4 μm, also increased. Transmission electron microscopy observation suggested that the broad luminescence was due to the dislocations induced in the Si matrix when the size of the embedded β-$FeSi_2$ particles was too large. Furthermore, the 1.5-μm PL intensity was observed to be strongly affected by MBE-Si growth rate. This is thought to be due to the strain induced in the β-$FeSi_2$ particles upon being embedded in the Si.
[DOI: 10.1063/1.1707233]

I. INTRODUCTION

Semiconducting iron disilicide (β-$FeSi_2$) has attracted much attention as a candidate for a Si-based light emitter with a wavelength ($\sim$1.5 μm) corresponding to optical fiber communication.[1] In 1997, Leong *et al.* reported the low-temperature electroluminescence from β-$FeSi_2$ precipitates embedded in a Si $p-n$ junction by ion-beam synthesis.[2] Room-temperature 1.6-μm light-emitting diodes (LEDs) with a β-$FeSi_2$ active region have been obtained from β-$FeSi_2$ particles embedded in the Si $p-n$ junction by IBS[3] and by molecular-beam epitaxy (MBE),[4,5] and very recently from p-type β-$FeSi_2$ films grown on n-type Si substrates using an rf magnetron sputtering technique.[6]

We have developed a technique for fabricating p-Si/β-$FeSi_2$-particles/n-Si (SFS) structures by reactive deposition epitaxy (RDE; Fe deposition on hot Si) for β-$FeSi_2$ and MBE for Si. To make an efficient LED with a β-$FeSi_2$ active region, the growth conditions for SFS structures must be optimized. Photoluminescence (PL) from β-$FeSi_2$ particles was observed to have a significant dependence on the growth conditions, including the Si substrate,[4] the growth temperatures of the MBE-Si overlayer for embedding β-$FeSi_2$ (see Ref. 5) and the boron-doped p-type Si capping layer,[7] and the annealing temperature after the MBE-Si overgrowth.[8] These growth conditions were optimized in our previous studies. However, the PL was observed to be dependent on the size of a β-$FeSi_2$ particle as well as on the Si growth rate for embedding β-$FeSi_2$.

The purpose of this work is to investigate the influence of the size of the β-$FeSi_2$ particle embedded in the Si matrices as well as the Si growth rate on the PL of β-$FeSi_2$.

II. EXPERIMENT

Samples were grown on n^+-type epitaxial Si (20 μm)/Czochralski n^+-Si(001) substrates using an ion-pumped MBE system equipped with a 30-keV reflection high-energy electron diffraction and electron-gun evaporation sources for Si and Fe. SFS structures were fabricated as follows. [100]-oriented β-$FeSi_2$ epilayers were grown on Si(001) substrates by RDE at 470 °C.[9] The thickness of the β-$FeSi_2$ layer was varied from 2 to 40 nm in order to vary the size of the β-$FeSi_2$ particle. The deposition rate of Fe was fixed at 0.6 nm/min using an electron impact emission spectroscopy sensor. The samples were then annealed *in situ* at 850 °C for 1 h to improve the crystal quality of the β-$FeSi_2$. The β-$FeSi_2$ crystals agglomerated into islands during this process,[10] due to the lattice mismatch (1%–2%) between the two materials. Consequently, a 0.3-μm-thick undoped Si layer was grown by MBE at 500 °C. The growth rate of the MBE-Si overlayer was 1.0 nm/min. In addition, SFS structures were prepared in order to examine the influence of the MBE-Si growth rate for embedding β-$FeSi_2$ in Si on the PL intensity. The thickness of the β-$FeSi_2$ film was fixed at 10 nm, while the growth rate of the undoped MBE-Si overlayer was varied from 2.6 to 7.9 nm/min by changing the input power of the electron-beam gun for Si. Finally, all of the samples were annealed at 900 °C in an Ar atmosphere for 14 h in order to improve the crystal quality. The final result was β-$FeSi_2$ particles embedded in a Si matrix.

PL measurements were performed at 77-K. The photoexcitation source was a 442-nm He-Cd laser. PL was analyzed by a 25-cm focal length single monochromator, detected by a liquid-nitrogen-cooled InP/InGaAs photomultiplier (Hamamatsu Photonics R5509-72) and amplified

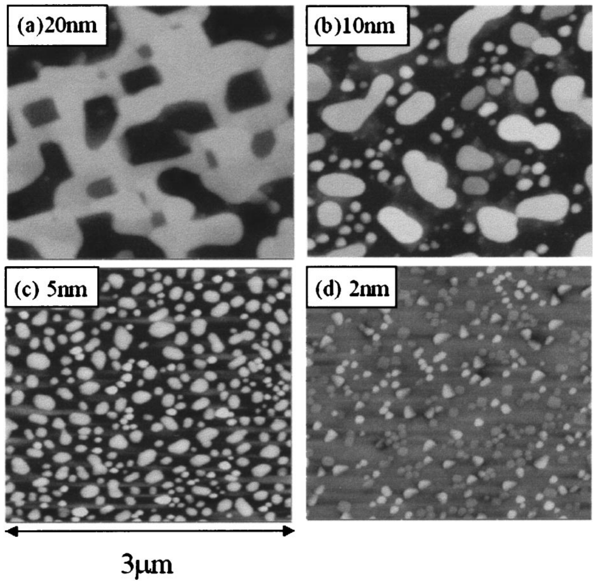

FIG. 1. AFM images of the β-$FeSi_2$ islands on Si(001) obtained after 850 °C annealing of (a) 20-, (b) 10-, (c) 5-, and (d) 2-nm-thick β-$FeSi_2$ films.

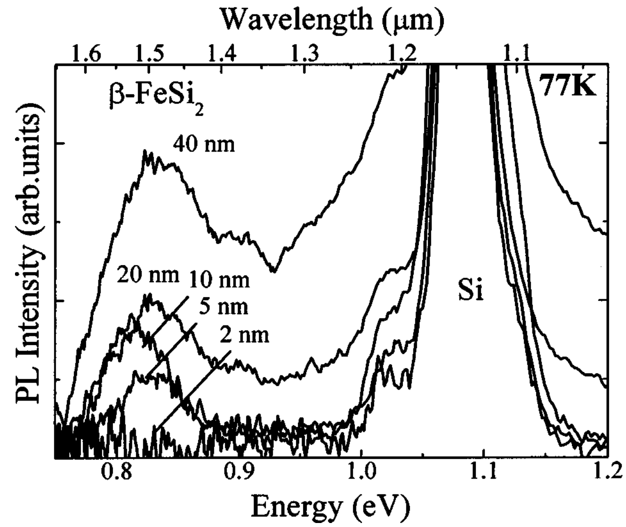

FIG. 2. 77-K PL spectra of samples grown with different β-$FeSi_2$ thicknesses.

by the lock-in technique. The surface morphologies of β-$FeSi_2$/Si were evaluated using atomic force microscopy (AFM). Cross-sectional and plan-view transmission electron microscopy (TEM) images were taken along the [110] and [001] azimuth of Si to visualize the SFS structure, respectively.

III. RESULTS AND DISCUSSION

A. Influence of β-$FeSi_2$ particle size on 1.5-μm PL emission

Figure 1 shows AFM images of the β-$FeSi_2$ islands on Si(001) obtained after 850 °C annealing of 20-, 10-, 5-, and 2-nm-thick β-$FeSi_2$ layers. The size of the β-$FeSi_2$ islands was large and inhomogeneous for surfaces from thick β-$FeSi_2$ films, as shown in Figs. 1(a) and 1(b), but the size decreased, becoming more uniform as the thickness of the β-$FeSi_2$ decreased, as shown in Figs. 1(c) and 1(d). Figure 2 shows 77-K PL spectra of the samples grown with different β-$FeSi_2$ thicknesses. The 1.5-μm PL intensity of β-$FeSi_2$ was observed to increase as the thickness of the β-$FeSi_2$ film increased. Interestingly, the broad background luminescence, ranging from 1.2 to 1.4 μm, also increased for the 20- and 40-nm-thick β-$FeSi_2$ samples. The TEM cross-sectional images, as shown in Fig. 3, revealed that dislocations were introduced around the β-$FeSi_2$ particles in the 40-nm-thick β-$FeSi_2$ sample. On the other hand, dislocations were not observed in the 5- and 10-nm-thick β-$FeSi_2$ samples. These results suggest that the broad background luminescence and the increase of 1.5-μm PL intensity observed for the 20- and 40-nm-thick β-$FeSi_2$ samples are related to dislocations induced in the Si matrix in initially thick films, which correspond to larger sized embedded β-$FeSi_2$ particles.

The dislocation-related PL in Si is known to consist of four lines.[11–14] They are labeled $D1$ (0.81 eV), $D2$ (0.87 eV), $D3$ ($\sim$0.95 eV), and $D4$ ($\sim$1.0 eV), and are radiative transitions via defect levels induced in the forbidden gap of Si. The increase of 1.5-μm PL intensity for the 5- and 10-nm-thick β-$FeSi_2$ samples was due to the increased number of carriers that recombined radiatively in β-$FeSi_2$ precipitates because of the increased volume of β-$FeSi_2$. On the other hand, the origin of the enhanced 1.5-μm PL for the 20- and 40-nm-thick β-$FeSi_2$ samples is thought to be the dislocation-related $D1$ line. The origin of the broad luminescence ranging from 1.2 to 1.4 μm is also thought to be the dislocation-related $D2$–$D4$ lines. The intensity of the $D2$–$D4$ lines was reported to decrease quickly with increasing temperature compared with the $D1$ line.[12,14] This is probably the reason we can see the broad luminescence instead of

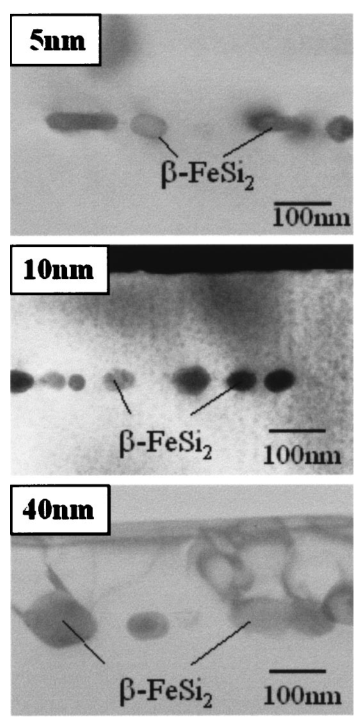

FIG. 3. Cross-sectional TEM images of SFS structures.

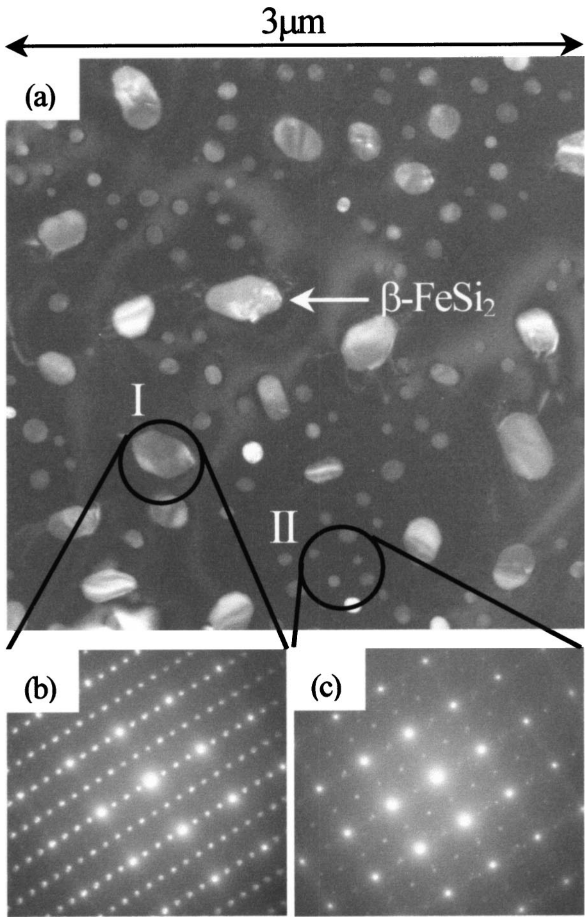

FIG. 4. (a) Plan-view TEM image of the 10-nm-thick β-$FeSi_2$ sample. TED patterns of (b) area I, containing one β-$FeSi_2$ island and (c) area II, containing several small β-$FeSi_2$ islands.

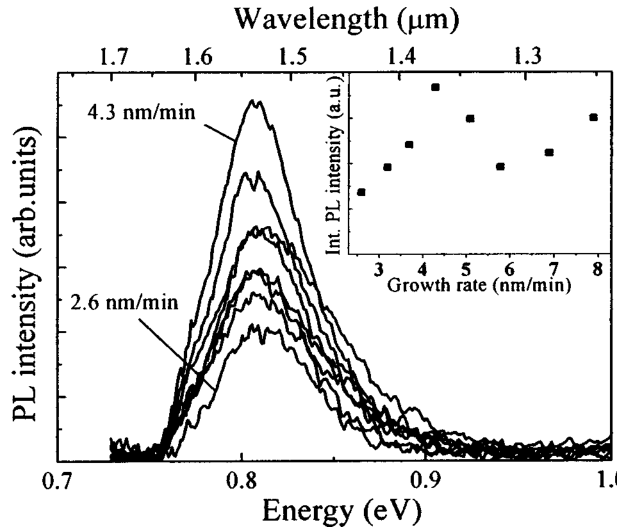

FIG. 5. 77-K PL spectra for samples with different Si growth rates for Si embedding β-$FeSi_2$ in Si. The inset shows the integrated PL intensity versus Si growth rate.

narrow $D2-D4$ lines in the range of 1.2 to 1.4 μm. On the basis of these results, it can be said that 1.5-μm PL from the SFS structures depends significantly on the particle size. Furthermore, optimum particles were obtained from a 10-nm-thick β-$FeSi_2$ films, which give a reasonable PL from the β-$FeSi_2$ particles without the broad background PL.[5]

Next, in order to investigate the lateral distribution and rotation of the β-$FeSi_2$ particles, plan-view TEM observation was performed on the 10-nm-thick β-$FeSi_2$ sample. As shown in Fig. 4(a), the size of β-$FeSi_2$ islands for this sample was irregular, like those in Fig. 1(b). Figures 4(b) and 4(c) are transmission electron diffraction (TED) images of area I, containing one β-$FeSi_2$ particle, and area II, containing several small β-$FeSi_2$ particles, respectively. The TEM patterns were taken along the [001] azimuth of Si. The fourfold symmetry of the Si(001) causes 90° rotational domains of [100]-oriented β-$FeSi_2$ in the epitaxial growth of β-$FeSi_2$ on Si(001).[15–17] The TED pattern, shown in Fig. 4(b), indicates the orientation alignment of β-$FeSi_2$(100)//Si(001) with either β-$FeSi_2$[010]//Si[110] or β-$FeSi_2$[001]//Si[110], whereas that in Fig. 4(c) indicates the coexistence of 90° rotational domains of β-$FeSi_2$(100)//Si(001) with β-$FeSi_2$[010] and [001]//Si[110].[17,18] These TED patterns reveal that the epitaxial orientation of β-$FeSi_2$ on Si(001) is preserved, even after aggregation of β-$FeSi_2$ films into particles upon high-temperature annealing.

B. Influence of Si growth rate on 1.5-μm PL emission

Figure 5 shows the dependence of the PL spectra on the MBE-Si growth rate for embedding β-$FeSi_2$ in Si. The 1.5-μm PL intensity of the β-$FeSi_2$ particles was observed to increase with the Si growth rate until 4.3 nm/min, but it tends to saturate with large scattering. The mechanism of the enhanced PL has yet to be clarified; however, it is thought to be related to the strain induced in the β-$FeSi_2$ particles embedded in Si matrix. It is important to note that β-$FeSi_2$ is an indirect bandgap semiconductor, and strain is required to transform it from an indirect to a direct bandgap semiconductor.[19–21] Recent reports demonstrated that 1.5-μm PL was not observed in β-$FeSi_2$ particles embedded in Si matrices at high temperatures (630–750 °C), but was observed in those at low temperatures (400–500 °C).[5] Furthermore, the *a* axis of the β-$FeSi_2$, from which PL was observed, was about 9% longer than both that of particles lacking PL and that of bulk β-$FeSi_2$. TEM observation revealed that the β-$FeSi_2$ islands embedded at 500 °C preserved an island-like shape after the MBE-Si growth and, after the 900 °C annealing, the β-$FeSi_2$ aggregated into particles. In contrast, β-$FeSi_2$ embedded at 750 °C aggregated into particles during the MBE-Si growth. These results suggest that it is when the island-like β-$FeSi_2$ embedded in Si aggregates into particles by the 900 °C annealing that strain is induced in the β-$FeSi_2$ particles. It is therefore very important to embed island-like β-$FeSi_2$ in Si by MBE. However, some of the β-$FeSi_2$ islands embedded in Si at 500 °C were observed to aggregate into particles just after the Si MBE.[5] This result suggests that the island-like β-$FeSi_2$ may aggregate into particles even at 500 °C during the MBE-Si growth.

The increased growth rate of MBE-Si shortened the growth time for embedding β-$FeSi_2$ in Si, and was thought to prevent the β-$FeSi_2$ islands from aggregating during the

MBE-Si growth and increase the number of island-like β-$FeSi_2$ embedded in Si. The increased growth rate of Si may hence increase the number of strained β-$FeSi_2$ particles obtained after the 900 °C annealing, which resulted in the observed PL enhancement. However, a too large growth rate of Si may lead to degradation of the crystalline quality of the MBE-Si layer itself, and thus the intensity of 1.5-μm PL is thought to saturate. Further TEM observation is required in order to clarify the relationship between the strain in the β-$FeSi_2$ particles and the Si growth rate.

IV. SUMMARY

Si/β-$FeSi_2$-particles/Si structures have been fabricated using RDE for β-$FeSi_2$ and MBE for Si. The 1.5-μm PL from β-$FeSi_2$ has been found to depend on the size of the β-$FeSi_2$ particle as well as the Si growth rate for embedding β-$FeSi_2$ in Si. Furthermore, the 1.5-μm PL intensity of β-$FeSi_2$ was observed to increase with the size of the embedded β-$FeSi_2$; however, the broad background luminescence, ranging from 1.2 to 1.4 μm, also increased. This broad luminescence is thought to be due to the dislocations induced in the Si matrix as the size of embedded β-$FeSi_2$ increases. In addition, the 1.5-μm PL intensity of β-$FeSi_2$ was observed to be strongly affected by the MBE-Si growth rate. This finding might be due to the strain induced in the β-$FeSi_2$ particles.

ACKNOWLEDGMENTS

TEM observation was supported by ''Nanotechnology Support Project'' of the Ministry of Education, Culture, Sports, Science and Technology (MEXT), Japan. This work was financially supported in part by Grants-in-Aid for Scientific Research (B)(12450137 and 12555084) from the MEXT of Japan, the TARA project of the University of Tsukuba, and the Industrial Technology Research Grant Program in 2002 from the New Energy and Industrial Technology Development Organization (NEDO) of Japan.

[1] M. C. Bost and J. E. Mahan, J. Appl. Phys. **58**, 2696 (1985).
[2] D. Leong, M. Harry, K. J. Reeson, and K. P. Homewood, Nature (London) **387**, 686 (1997).
[3] M. A. Lourenco, T. M. Butler, A. K. Kewell, R. M. Gwilliam, K. J. Kirkby, and K. P. Homewood, Jpn. J. Appl. Phys. **40**, 4041 (2001).
[4] T. Suemasu, Y. Negishi, K. Takakura, and F. Hasegwa, Jpn. J. Appl. Phys. **39**, L1013 (2000).
[5] T. Suemasu, Y. Negishi, K. Takakura, F. Hasegawa, and T. Chikyow, Appl. Phys. Lett. **79**, 1804 (2001).
[6] S. Chu, T. Hirohda, K. Nakajima, H. Kan, and T. Hiruma, Jpn. J. Appl. Phys. **41**, L1200 (2002).
[7] Cheng Li, T. Ohtsuka, Y. Ozawa, T. Suemasu, and F. Hasegawa, J. Appl. Phys. **94**, 1518 (2003).
[8] T. Suemasu, Y. Iikura, K. Takakura, and F. Hasegawa, J. Lumin. **87–89**, 528 (2000).
[9] M. Tanaka, Y. Kumagai, T. Suemasu, and F. Hasegawa, Jpn. J. Appl. Phys. **36**, 3620 (1997).
[10] T. Suemasu, M. Tanaka, T. Fujii, S. Hashimoto, Y. Kumagai, and F. Hasegawa, Jpn. J. Appl. Phys. **36**, L1225 (1997).
[11] D. A. Drozdov, A. A. Patrin, and V. D. Tkachev, Sov. Phys. JETP **23**, 597 (1976).
[12] B. Suezawa, Y. Sasaki, and K. Sumio, Phys. Status Solidi A **79**, 173 (1983).
[13] R. Sauer, J. Weber, J. Stolz, E. Weber, K. Kusters, and H. Alexander, Appl. Phys. A: Solids Surf. **36**, 1 (1985).
[14] V. V. Kveder, E. A. Steinman, S. A. Shevchenko, and H. G. Grimmeiss, Phys. Rev. B **51**, 10520 (1995).
[15] J. E. Mahan, K. M. Geib, G. Y. Robinson, R. G. Long, X. Yan, G. Bai, M. A. Nicolet, and M. Nathan, Appl. Phys. Lett. **56**, 2126 (1990).
[16] J. E. Mahan, V. L. Thanh, J. Chevrier, I. Berbezier, J. Derrien, and R. G. Log, J. Appl. Phys. **74**, 1747 (1993).
[17] K. M. Geib, J. E. Mahan, R. G. Long, M. Nathan, and G. Bai, J. Appl. Phys. **70**, 1730 (1991).
[18] H. U. Nissen, E. Müller, H. R. Deller, and H. V. Känel, Phys. Status Solidi A **150**, 395 (1995).
[19] S. J. Clark, H. M. Al-Allak, S. Brand, and R. A. Abram, Phys. Rev. B **58**, 10389 (1998).
[20] D. B. Migas and L. Miglio, Phys. Rev. B **62**, 11063 (2000).
[21] K. Yamaguchi and K. Mizushima, Phys. Rev. Lett. **86**, 6006 (2001).